# MODELLING OF BEAM EXCITED BY PIEZOELECTRIC ACTUATORS IN VIEW OF TACTILE APPLICATIONS

Clément Nadal, Christophe Giraud-Audine, Frédéric Giraud, Michel Amberg, Betty Lemaire-Semail

# MODELLING OF BEAM EXCITED BY PIEZOELECTRIC ACTUATORS IN VIEW OF TACTILE APPLICATIONS

C. Nadal, C. Giraud-Audine, F. Giraud, M. Amberg and B. Lemaire-Semail

L2EP-IRCICA, Université de Lille 1, 50 avenue Halley, Villeneuve d'Ascq, France
e-mail : clement.nadal@ircica.univ-lille1.fr

**Abstract -** This paper deals with an one-dimensional semi-analytical modelling of the vibratory behaviour of a rectangular beam excited by several piezoelectric ceramics glued on its lower face. The establishment of the equations of motion is guaranteed by the application of Hamilton's principle. From this approach, it results an accurate knowledge on the mode shape in function of the geometry, the structure and the positions of the piezoelectric actuators. This approach deployed on a simple case falls within a general process of the tactile surfaces optimization. This article shows that there is a trade-off between the optimization of the homogeneity of the tactile stimulation and the electromechanical coupling factor.

**Keyword -** Semi-analytical modelling, Piezoelectricity, Tactile applications, Hamilton's principle.

## 1 INTRODUCTION

During the last decade, a noticeable interest has been demonstrated for the sense of touch in the human-computer interaction, owing to its importance in the perception of our world by the manipulation and the identification of the objects surrounding us. In order to enhance the interaction between the user and the communicating device, it is considered to provide to the former a rendering of tactile sensations matching the actions he performs. In this sense, the field of tactile feedback has been emphasized by the emergence of several technologies. One of them uses lateral forces which create the illusion of fine textures and surface features [1]. Many haptic surfaces have been realized to take advantage of this illusion. Watanabe and Fukui [2] developed the first ultrasonic vibrating plate, with resonant frequency of 75.6 kHz and amplitude 2 μm, able to control the roughness surface displayed to a bare finger. The main idea was to use the reduction of the effective friction force thanks to an air film between the vibrating plate and the user's finger, the so-called *squeeze film effect*. Biet et al. [3] used a monomorph composed of an array of piezoelectric actuators bonded on the lower face of a metallic plate to generate out-of-plane vibrations of 1 μm amplitude at a 30.5 kHz resonant frequency. A circular variant of such a device was developed by Winfield et al. [4] who mounted a glass disk on a circular piezoelectric actuator. In a near future, these technologies will be destined to equip general public systems with tactile screen (smart phones, tablet computers, laptops, remote controls,

etc.). In fact, their implementation in a limited environment gives rise to optimization questions in terms of, especially, energy consumption and mass of used piezoelectric ceramics. A first attempt has been carried out by Sergeant et al. [5] who determined the optimal dimensions of the resonator and the ceramics composing the device in order to obtain a maximal deflection with a minimal supply voltage.

In this paper, a different problem is addressed. Indeed, it is shown [3] that an homogeneous deformation is required in order to get an uniform tactile stimulus thus, the goal is to obtain such a condition, with a minimal amount of ceramics and enough amplitude. Moreover, the location of the piezoelectric ceramic actuators is also optimized to select specific mode shapes to realize a satisfactory stimulation. Briefly put, the deformation should be as homogeneous as possible in order to obtain an uniform tactile stimulus all over the plate surface while having the largest conversion factor.

To achieve this, a semi-analytical model is developed in this paper. Its main aim is to study the influence of the ceramics on the resonant frequencies (the squeeze film effect being effective for a frequency greater than 25 kHz [3]) and the mode shapes, especially in terms of promotion and uniformity. Based on some well-known assumptions used for the study of laminated structures, such a modelling is commonly carried out for the active vibration control. For instance, Ducarne et al. [6] optimize the placement and the dimensions of shunted piezoelectric ceramics dedicated to

vibration reduction. Numerical methods have been also validated for the understanding of the dynamic of these active structures (see e.g. [7]). In this paper, a generalized model of a free-free beam excited by $n_a$ piezoelectric actuators bonded on its lower faces, defining a non-symmetric geometry, is detailed. In fact, in this article, the geometry and the different assumptions enabling its formulation will be firstly specified. Then, the equations of motion will be deduced from the application of Hamilton's principle. Finally, example structures composed of two ceramics will be simulated and studied in terms of homogeneity and promotion of mechanical mode shapes.

## 2 SEMI-ANALYTICAL MODELLING

### 2.1 GEOMETRY AND ASSUMPTIONS

The semi-analytical modelling developed below relies on a geometry of a rectangular cross-section beam composed of $N$ parts in the longitudinal direction and excited on its back, as illustrated by Fig. 1, by $n_a$ piezoelectric ceramics behaving like actuators. The beam is supposed to be a parallelepiped of dimensions $L_b \times w_b \times h_b$. The $i^{\text{th}}$ actuator is a parallelepiped of the same width than the beam $w_a = w_b$, a length $L_a^{(i)}$ and a thickness $h_a^{(i)}$. These ceramics are polarized along the $z$-axis and are supplied from their lower and upper faces in order to preferentially use a transverse piezoelectric coupling (variation of the sample length along the $x$-axis perpendicular to the polarization direction). Thereafter, the Cartesian coordinate system is chosen and its origin is put at the center of the beam. Moreover, the $i^{\text{th}}$ ceramic actuator are located by the set of abscissae $(x_{a-}^{(i)}, x_{a+}^{(i)})$. The modelling of the beam dynamic is based on the Classical Laminated Plate Theory (CLPT) (see e.g. [8], Sec. 3.3, pp. 112-114) adapted to an one-dimensional problem. The main hypothesis of this approach are reminded below to which the electrical assumptions have been added.

M.1 The thicknesses of the beam $h_b$ and the ceramics $(h_a^{(i)})_{i \in [\![1, n_a]\!]}$ are supposed to be small compared to the main dimension of the beam.

M.2 Any plane parallel to the $xz$-plane is supposed to be a symmetry plane for the problem geometry. Thus, all mechanical and electrical quantities are independent of the space variable $y$. Furthermore, the displacement along the $y$-axis, $u_y$, the transverse strain and stress, $S_{yy}$ and $T_{yy}$ respectively, and the shear strains around $x$- and $z$-axis, $S_{yz}$ and $S_{xy}$ respectively, are neglected ($u_y = 0$, $S_{yy} = S_{yz} = S_{xy} = 0$ and $T_{yy} = 0$).

M.3 All cross-sections perpendicular to the neutral axis remain planar and perpendicular after deformation. The shear in the $xy$-plane is implicitly neglected ($S_{xz} = 0$).

M.4 The pure flexure case being the main point of interest in this study, it is assumed that the normal extension is negligible during the deformation. The deformed beam does not consequently stretch along the $z$-axis resulting in zero normal strain ($S_{zz} = 0$). The normal stress is also neglected ($T_{zz} = 0$).

M.5 The ceramics are perfectly glued on the beam and the thickness of the bonding layer is negligible so it is not taken into account. Moreover, the displacements are supposed to be common to the beam and the ceramics.

M.6 The beam is supposed to be free on its ends which implies that the axial force $N$, the bending moment $M$ and the shear force $Q = -M_{,x}$ (the symbol $(.)_{,x}$ denotes a partial derivative with respect to the variable $x$) are null at $x = \pm L_b/2$.

E.1 The ceramic actuators being assumed reasonably thin and supplied from its lower and upper faces, the electric field $\mathbf{E}$, deriving from the electric potential $\phi$, is supposed to be only orientated along the $z$-axis so much that :

$$\mathbf{E} = \begin{bmatrix} 0 & 0 & -\phi_{,z} \end{bmatrix}^{\mathsf{T}} \tag{1}$$

where the superscripted $\mathsf{T}$ indicates matrix transposition.

E.2 The $i^{\text{th}}$ ceramic actuator is supposed to be respectively connected to the potential $v_a^{(i)}(t)$ and the ground on its lower and upper faces so that :

$$\begin{cases} \phi(x, z = -h_b/2 - h_a^{(i)}, t) = v_a^{(i)}(t) \\ \phi(x, z = -h_b/2, t) = 0 \end{cases} \tag{2}$$

### 2.2 CONSTITUTIVE RELATIONSHIPS

The material of the beam is supposed to be linear, isotropic and homogeneous, therefore the strain $\mathbf{S}$ and stress $\mathbf{T}$ vectors are linked by the Hooke's law. From the assumptions (M.2), (M.3) and (M.4), the constitutive relationship reduces to the following equation :

$$\mathbf{T} = [c]\mathbf{S} \quad \Longleftrightarrow \quad T_{xx} = E_b S_{xx} \tag{3}$$

where $E_b$ is the Young's modulus of the material constituting the beam.

Due to the assumptions (M.2), (M.3), (M.4) and (E.1), the equations describing the piezoelectric behaviour (see e.g. [9], Sec. 1.2.1, pp. 11, eq. 1.2.32) reduce to :

$$\begin{aligned} T_{xx} &= \bar{c}_{11}^E S_{xx} - \bar{e}_{31} E_z \\ D_z &= \bar{e}_{31} S_{xx} + \bar{\varepsilon}_{33}^S E_z \end{aligned} \tag{4}$$
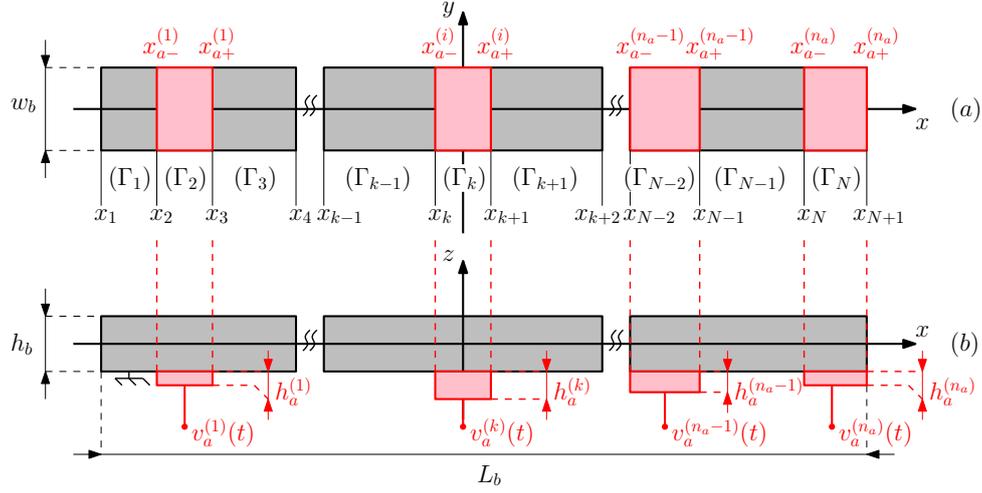
Fig. 1. Bottom view (a) and cross view (b) of a beam excited by $n_a$ piezoelectric actuators

where $\bar{c}_{11}^E$, $\bar{e}_{31}$ and $\bar{\varepsilon}_{33}^S$ are respectively the transverse stiffness at constant electric field, the piezoelectric co-efficient and the longitudinal permittivity at constant strain. The bar symbol on these structural coefficients denotes the specific value of the transverse coupling mode expressed as follows :

$$\bar{c}_{11}^E = \frac{1}{s_{11}^E} \; ; \; \bar{e}_{31} = \frac{d_{31}}{s_{11}^E} \; ; \; \bar{\varepsilon}_{33}^S = \varepsilon_{33}^T(1 - k_{31}^2) \quad (5)$$

where $k_{31}$ is the transverse piezoelectric coupling factor.

### 2.3 KINEMATIC AND ELECTRICAL QUANTITIES

The displacement corresponding to the mechanical assumptions are (see e.g. [8], Sec. 3.3.2, p. 114, eq. 3.3.2) :

$$\mathbf{u} = \begin{bmatrix} u(x,t) - zw_{,x}(x,t) \\ 0 \\ w(x,t) \end{bmatrix} \quad (6)$$

where $u$ and $w$ characterize the displacement fields in longitudinal extension and in flexure, respectively. Note that the coupling between $u$ and $w$ implicitly enables to take into account the variation of the neutral axis position arising from asymmetry introduced by the gluing of the ceramics of one side of the beam. The strain vector $\mathbf{S}$ is besides deduced from the previous relationship by applying the displacement gradient in the framework of linear elasticity so much that the only nonzero component of this vector is written as follows :

$$S_{xx}(x,z,t) = u_{,x}(x,t) - zw_{,xx}(x,t) \quad (7)$$

Concerning the electrical quantities, for each ceramic actuator, it follows from (1), (7) and (4) that the electric displacement field is given by

$$D_z = \bar{e}_{31}(u_{,x} - zw_{,xx}) - \bar{\varepsilon}_{33}^S \phi_{,z} \quad (8)$$

Besides, since $\mathbf{D}$ is conservative, $D_{z,z} = 0$. Using this condition and (2), the electric potential in the $i$th actuator can be deduced and the $z$-axis component of the electric field is consequently written as follows :

$$E_z(x,z,t) = \frac{v_a^{(i)}(t)}{h_a^{(i)}} + \frac{\bar{e}_{31}}{\bar{\varepsilon}_{33}^S}\left(z - h_{ma}^{(i)}\right)w_{,xx}(x,t) \quad (9)$$

where $h_{ma}^{(i)} = -(h_b + h_a^{(i)})/2$ is the height of the center of the $i$th ceramic actuator.

### 2.4 APPLICATION OF HAMILTON'S PRINCIPLE

According to [10] (Sec. 4.8, pp. 121-124), a general form of Hamilton's principle applied to a piezoelectric system is

$$\int_{t_1}^{t_2} (\delta\overline{\mathcal{L}} + \delta\mathcal{W}_{ext})\mathrm{d}t = 0 \quad (10)$$

where $\delta\overline{\mathcal{L}}$ and $\delta\mathcal{W}_{ext}$ are respectively the variations on the time interval $[t_1, t_2]$ of the modified Lagrangian $\overline{\mathcal{L}}$ and the work done by external forces and sources which is expressed as follows :

$$\delta\mathcal{W}_{ext} = \int_{\Gamma_b} n\delta u\mathrm{d}\Gamma + \int_{\Gamma_b} p\delta w\mathrm{d}\Gamma + \sum_{i=1}^{n_a} i_a^{(i)}\delta\lambda_a^{(i)} \quad (11)$$

where $n(x,t)$ and $p(x,t)$ are respectively the linear density of axial and normal forces. The modified Lagrangian $\overline{\mathcal{L}}$ is the sum of the Lagrangian $\mathcal{L}$ of the global structure to which Lagrange multipliers (for more details see e.g. [12], Sec. II.5, pp. 43-48) have been added in order to respect the $3(N-1)$ kinematic conditions at the interfaces between each section $\Gamma_k$ which are expressed as follows :

$$\begin{cases} u(x = x_k^-, t) = u(x = x_k^+, t) \\ w(x = x_k^-, t) = w(x = x_k^+, t) \\ w_{,x}(x = x_k^-, t) = w_{,x}(x = x_k^+, t) \end{cases} \quad (12)$$

The Lagrangian $\mathcal{L}$ of the studied system is the sum of $n_a + 1$ contributions corresponding to the actuators and the beam so much that :

$$\mathcal{L} = \mathcal{L}_b + \sum_{i=1}^{n_a} \mathcal{L}_a^{(i)} \tag{13}$$

where $\mathcal{L}_b$ is the Lagrangian of the beam which is classically written as follows :

$$\mathcal{L}_b = \frac{1}{2} \int_{\Gamma_b} \left[ \mathcal{M}_b(\dot{u}^2 + \dot{w}^2) - \mathcal{K}_b u_{,x}^2 - \mathcal{D}_b w_{,xx}^2 \right] \mathrm{d}\Gamma \tag{14}$$

where $\Gamma_b = \bigcup_{k=1}^N \Gamma_k$ symbolises the neutral axis of the bare beam and $\mathcal{M}_b$, $\mathcal{K}_b$ and $\mathcal{D}_b$ are respectively the linear mass, axial stiffness and flexural rigidity of the beam defined by

$$\mathcal{M}_b = \rho_b w_b h_b \; ; \; \mathcal{K}_b = E_b w_b h_b \; ; \; \mathcal{D}_b = E_b w_b \frac{h_b^3}{12} \tag{15}$$

and $\mathcal{L}_a^{(i)}$ is the Lagrangian of the $i^{\text{th}}$ ceramic actuator defined as follows :

$$\begin{aligned}
\mathcal{L}_a^{(i)} = \frac{1}{2} \int_{\Gamma_a^{(i)}} &\left[ \mathcal{M}_a^{(i)}(\dot{u}^2 + \dot{w}^2) \right. \\
&- \mathcal{K}_a^{(i)} u_{,x}^2 - 2\mathcal{J}_a^{(i)} u_{,x} w_{,xx} - \mathcal{D}_a^{(i)} w_{,xx}^2 \\
&\left. + 2 \left[ \psi_a^{(i)} u_{,x} + \varphi_a^{(i)} w_{,xx} \right] v_a^{(i)} + \mathcal{C}_a^{(i)}(v_a^{(i)})^2 \right] \mathrm{d}\Gamma
\end{aligned} \tag{16}$$

where $\mathcal{M}_a^{(i)} = \rho_a^{(i)} w_a h_a^{(i)}$ is the linear mass of the $i^{\text{th}}$ ceramic actuator and $\mathcal{K}_a^{(i)}$, $\mathcal{J}_a^{(i)}$, $\mathcal{D}_a^{(i)}$ are respectively the linear axial stiffness, elastic coupling factor, flexural rigidity defined by

$$\mathcal{K}_a^{(i)} = \bar{c}_{11}^E w_a h_a^{(i)} \; ; \; \mathcal{J}_a^{(i)} = -\bar{c}_{11}^E w_a h_a^{(i)} h_{ma}^{(i)} \tag{17}$$

$$\mathcal{D}_a^{(i)} = \bar{c}_{11}^E w_a h_a^{(i)} \left[ \frac{(h_a^{(i)})^2}{12(1 - k_{31}^2)} + (h_{ma}^{(i)})^2 \right] \tag{18}$$

$\psi_a^{(i)}$, $\varphi_a^{(i)}$ and $\mathcal{C}_a^{(i)}$ are the linear axial and flexural electromechanical coupling factors and the clamped capacitance whose expression are respectively:

$$\psi_a^{(i)} = \bar{e}_{31} w_a \; ; \; \varphi_a^{(i)} = -\bar{e}_{31} w_a h_{ma}^{(i)} \; ; \; \mathcal{C}_a^{(i)} = \bar{\varepsilon}_{33}^S \frac{w_a}{h_a^{(i)}} \tag{19}$$

Applying the rules of variational calculus (see e.g. [10], Sec. 4.8, pp. 121-124), the stationary of the definite integral (10) leads to the equations governing the system dynamic and additionally gives the $3(N-1)$ extra continuity relationships by removing the Lagrange multipliers. These foregoing equations affect the axial force $N$, the bending moment $M$ and the shear force $Q$ which may be expressed in a general way on the section $\Gamma_k = \Gamma_a^{(i)}$ as follows :

• Continuity relationships at $x = x_k$

$$\begin{cases}
N_{k-1}(x_k, t) = N_k(x_k, t) - N_a^{(i)}(t) \\
M_{k-1}(x_k, t) = M_k(x_k, t) - M_a^{(i)}(t) \\
Q_{k-1}(x_k, t) = Q_k(x_k, t)
\end{cases} \tag{20}$$

• Continuity relationships at $x = x_{k+1}$

$$\begin{cases}
N_k(x_{k+1}, t) - N_a^{(i)}(t) = N_{k+1}(x_{k+1}, t) \\
M_k(x_{k+1}, t) - M_a^{(i)}(t) = M_{k+1}(x_{k+1}, t) \\
Q_k(x_{k+1}, t) = Q_{k+1}(x_{k+1}, t)
\end{cases} \tag{21}$$

It should be noted that the beam vibration is locally induced at the ends of each ceramic actuator by means of an axial force $N_a^{(i)}(t) = \psi_a^{(i)} v_a^{(i)}(t)$ and a bending moment $M_a^{(i)}(t) = \varphi_a^{(i)} v_a^{(i)}(t)$.

In a pure flexure case, where an uncoupling of the axial $u$ and flexural $w$ motions has been acted (for more details see [6], Sec. 2.2.2, p. 3290), the resulting mechanical equations are written on each section $(\Gamma_k)_{k \in [\![1,N]\!]}$ as follows :

$$\forall x \in \Gamma_k \; , \; \mathcal{M}_k \ddot{w}(x, t) + \mathcal{D}_k w_{,xxxx}(x, t) = p(x, t) \tag{22}$$

where $\mathcal{M}_k$ and $\mathcal{D}_k$ are the linear mass and flexural rigidity of the section $\Gamma_k$ given by

$$\mathcal{M}_k = \begin{cases} \mathcal{M}_b + \mathcal{M}_a^{(i)} & \text{, if } \Gamma_k = \Gamma_a^{(i)} \\ \mathcal{M}_b & \text{, otherwise} \end{cases} \tag{23}$$

and

$$\mathcal{D}_k = \begin{cases} \mathcal{D}_{ba}^{(i)} - \left[ \mathcal{J}_a^{(i)} \right]^2 / \mathcal{K}_{ba}^{(i)} & \text{, if } \Gamma_k = \Gamma_a^{(i)} \\ \mathcal{D}_b & \text{, otherwise} \end{cases} \tag{24}$$

with $\mathcal{K}_{ba}^{(i)} = \mathcal{K}_b + \mathcal{K}_a^{(i)}$ and $\mathcal{D}_{ba}^{(i)} = \mathcal{D}_b + \mathcal{D}_a^{(i)}$. From the equation (22), the determination of eigenmodes is carried out for a free beam with short circuited ceramic actuators. Assuming that the mechanical and electrical quantities harmonically evolve, which means for the deflection that $w(x, t) = \underline{w}(x) \exp(j\omega t)$ with $j^2 = -1$ and $\underline{w}(x)$ its amplitude at the angular frequency $\omega$, it leads to :

$$\forall x \in \Gamma_k \; , \; \underline{w}_{,xxxx}(x) - (\alpha_k k_b)^4 \underline{w}(x) = 0 \tag{25}$$

where $k_b = (\omega^2 \mathcal{M}_b / \mathcal{D}_b)^{1/4}$ is the wave vector related to the flexural modes of the bare beam and $\alpha_k = [(\mathcal{M}_k / \mathcal{M}_b)/(\mathcal{D}_k / \mathcal{D}_b)]^{1/4}$. The general solution of this system of equations is written as a linear combination of Duncan's function defined for $i = 1, 2$ by $[c_i, s_i] = [\cosh + (-1)^{i+1} \cos, \sinh + (-1)^{i+1} \sin]$. The use of the boundary conditions (M.6) and the continuity relationships (12), (20) and (21) leads to a system of $4N$ equations which degenerates for particular frequencies defining the resonances. Furthermore, it enables to find the mode shapes $\phi^{(n)}$ up to a multiplicative constant which can be set using the modal mass normalization criterion given by the following relationship :

$$\forall n \in \mathbb{N}^* \; , \; \sum_{k=1}^N \int_{\Gamma_k} \mathcal{M}_k \left[ \phi^{(n)}(x) \right]^2 \mathrm{d}x = 1 \tag{26}$$

## 3  SIMULATION

The initial aim of such a study is to quantify the influence of the ceramics on the flexural mode shapes, both the impact of their dimensions, their constitution and one of their position, even if no damping has been considered in the semi-analytical modelling. The case of a beam excited by two ceramics glued with the same polarization direction is hold and the parameters used for the simulation are listed in Table I. In light of these considerations, a preliminary parametric study has been carried out in order to determine the ceramic positions on the host structure optimizing the energy conversion (all others things being equal). The idea was to study, for each mode shape, the evolution of the effective electromechanical coupling coefficient (EEMCC) $k_{\text{eff}}^{(n)}$ against the set of parameters $(\chi_a^{(1)}, \chi_a^{(2)}) = (x_{a-}^{(1)}, x_{a-}^{(2)})/L_b$ defining the ceramic positions. In piezoelectricity, $k_{\text{eff}}^{(n)}$ is the classical relevant parameter enabling to characterize the energy conversion, acting in the present case between the ceramics and the host structure. It is defined by the IEEE standards [13] as follows :

$$k_{\text{eff}}^{(n)} = \sqrt{1 - \left[ f_{\text{sc}}^{(n)} / f_{\text{oc}}^{(n)} \right]^2} \qquad (27)$$

where $f_{\text{sc}}^{(n)}$ and $f_{\text{oc}}^{(n)}$ are the resonant frequencies of the vibrating system while the ceramic actuators are respectively in short-circuit and open circuit. For example, $k_{\text{eff}}^{(n)}$ is depicted in Fig. 2 as a function of $\chi_a^{(1)}$ and $\chi_a^{(2)}$ for the fifth mode in flexure. The central band correspond with the overlapping of the ceramics which has no physical reality. The symmetry of the pattern is due to the equivalent characteristics of both ceramics.

I. Geometrical and structural parameters

|  |  | Definition | Value | Unit |
|---|---|---|---|---|
| $L_b$ |  | Length | 100 | mm |
| $w_b$ |  | Width | 7 | mm |
| $h_b$ |  | Thickness | 1.94 | mm |
| $\rho_b$ |  | Mass density | 2700 | kg/m$^3$ |
| $E_b$ |  | Young's modulus | 69.0 | GPa |
| $L_a^{(i)}$ |  | Length | 11 | mm |
| $w_a^{(i)}$ |  | Width | 7 | mm |
| $h_a^{(i)}$ |  | Thickness | 1 | mm |
| $\rho_a^{(i)}$ |  | Mass density | 8000 | kg/m$^3$ |
| $s_{11}^E$ |  | Compliance | 17 | µm$^2$/N |
| $-d_{31}$ |  | Piezo. coef. | 260 | pm/V |
| $\varepsilon_{33}^T/\varepsilon_0$ |  | Relative Permittivity | 5000 |  |
| $k_{31}$ |  | Coupling factor | 0.390 |  |

This figure is used to deduce the location of the ceramics promoting a particular mode. For instance, the
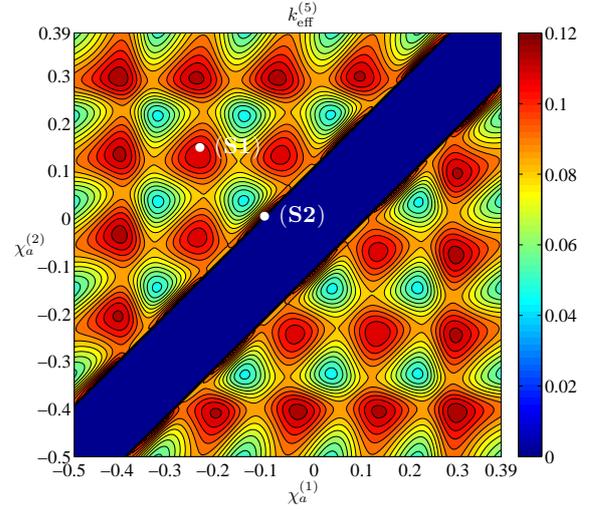


Fig. 2. EEMCC for the fifth flexural mode shape.

geometry defined by $(\chi_a^{(1)}, \chi_a^{(2)}) = (-0.250, 0.150)$, named thereafter (S1), specifically promotes the flexural mode of rank 5. For purpose of comparison, another geometry named (S2) and defined by $(\chi_a^{(1)}, \chi_a^{(2)}) = (-0.115, 0.005)$ globally promotes the modes of rank 1, 3 and 5. These geometries were manufactured and the table II shows the good agreement between predicted and measured resonant frequencies.

II. Theoretical and experimental resonant frequencies of both structures (S1) and (S2).

| $f_r^{(n)}$ (Hz) | Structure (S1) | | Structure (S2) | |
|---|---|---|---|---|
| Mode rank | Th. | Exp. | Th. | Exp. |
| 1 | 1074 | 1045 | 1104 | 1086 |
| 3 | 5488 | 5348 | 5699 | 5519 |
| 5 | 13978 | 13185 | 13828 | 13217 |

The modelling developed in the paper can also be used to compare the mode shapes of both geometries (see Fig. 3). This figure shows the fifth mode in flexure for each structure and highlights the fact that the mode shape is modified by the ceramics. However, in tactile applications, the user can be sensible to modal deformation. Indeed, the stimulation depends on the vibration amplitude under the fingertip [3]. This influence can be quantified in terms of homogeneity of the vibration using the minimization of the following criterion, defined for $n \in \mathbb{N} \backslash \{0, 1\}$ by

$$\sigma_H^{(n)} = \sum_{\substack{i=1 \\ j<i}}^{n} \frac{\left| \left| \phi^{(n)}(\chi_i^*) \right| - \left| \phi^{(n)}(\chi_j^*) \right| \right|}{\binom{n}{2} \max_{k \in [\![1,n]\!]} \left| \phi^{(n)}(\chi_k^*) \right|} \qquad (28)$$

where $\binom{n}{k}$ is the binomial coefficient and $(\chi_k^*)_{k \in [\![1,n]\!]}$ is the vector of dimensionless abscissae matching the local mode shape extrema.
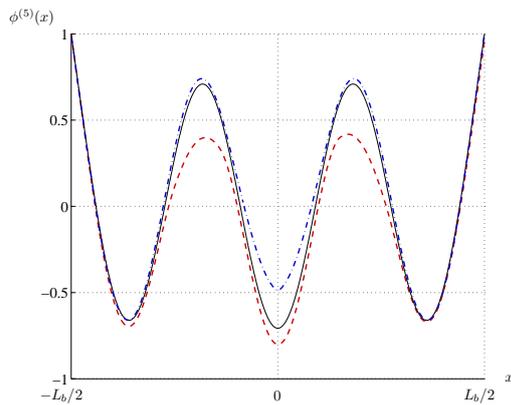
Fig. 3. Fifth mode shape for the structures (S1) (in dashed line), (S2) (in dash-dotted line) and the bare beam (solid line).

For both structures, $\sigma_H^{(5)}$ is respectively equal to 0.27 for (S1) and 0.15 for (S2) with an EEMCC pretty much equal ($k_{\text{eff}}^{(5)} \simeq 0.10$). Hence, the design which optimizes the energy conversion for mode 5 is not for the homogeneity. This conclusion can be generalized for flexural mode shapes with a rank $n \geq 3$.

## 4  CONCLUSION

This paper has presented an one-dimensional semi-analytical modelling of a beam excited by ceramic actuators of any number. This approach is a first step in view of an optimization of tactile devices using the squeeze film effect. This phenomenon is generated between a vibrating plate, activated by piezoelectric ceramics, and an user's finger. It is thus important to precisely know the actuators impact on the dynamic of such a structure. From the study of two structures composed of two ceramic actuators, this article has highlighted a trade-off to act between the promotion of a mechanical mode shape and its homogeneity which may be unacceptable for tactile feedback devices if it is not provided. For future works, the influence of the function sensor accomplished by extra ceramics will be studied. An extension to a 2D model is also envisaged.

### REFERENCES

[1] M. Wiertlewski, J. Lozada and V. Hayward, *The Spatial Spectrum Of Tangential Skin Displace-*

*ment Can Encode Tactual Texture*, IEEE Transactions on Robotics, Vol. 27, No. 3, pp. 461-472, June 2011.

[2] T. Watanabe and S. Fukui, *A Method for Controlling Tactile Sensation of Surface Roughness Using Ultrasonic Vibration*, 1995 IEEE International Conference on Robotics and Automation, Nagoya, Japan, Vol. 1, pp. 1134-1139, May 21-27, 1995.

[3] M. Biet, F. Giraud and B. Lemaire-Semail, *Implementation of Tactile Feedback by Modifying the Perceived Friction*, The European Physical Journal Applied Physics, Vol. 43, No. 1, pp. 123-135, July 2008.

[4] L. Winfield, J. Glassmire, J.E. Colgate and M. Peshkin, *T-PaD: Tactile Pattern Display through Variable Friction Reduction*, 2007 World Haptics Conference, Tsukuba, Japan, pp. 421-426, March 22-24, 2007.

[5] P. Sergeant, F. Giraud and B. Lemaire-Semail, *Geometrical optimization of an ultrasonic tactile plate*, Sensors and Actuators A: Physical, Vol. 161, No. 1-2, pp. 91-100, June 2010.

[6] J. Ducarne, O. Thomas and J.-F. Deü, *Placement and dimension optimization of shunted piezoelectric patches for vibration reduction*, Journal of Sound and Vibration, Vol. 331, No. 14, pp. 3286-3303, July 2012.

[7] C. Maurini, M. Porfiri and J. Pouget, *Numerical methods for modal analysis of stepped piezoelectric beams*, Journal of Sound and Vibration, Vol. 298, No. 4-5, pp. 918-933, December 2006.

[8] J.N. Reddy, *Mechanics of Laminated Composite Plates and Shells: Theory and Analysis - Second Edition*, CRC Press, 2003.

[9] J. Yang, *Analysis of Piezoelectric Devices*, World Scientific Publishing, 2006.

[10] A. Preumont, *Mechatronics: Dynamics of Electromechanical and Piezoelectric Systems*, Springer, 2006.

[11] T. Ikeda, *Fundamentals of Piezoelectricity*, Oxford University Press, 1996.

[12] C. Lanczos, *The Variational Principles of Mechanics - Fourth Edition*, Dover Publication, 1986.

[13] *IEEE Standard on Piezoelectricity* ANSI/IEEE Std 176-1987, 1988.